STUDIES OF FLOW PROBLEMS WITH THE SIMULATOR SHAFT78

K. Pruess, R.C. Schroeder, J. Zerzan
'Lawrence Berkeley Laboratory
University of California
Berkeley, California 94720

In recent years, a number of numerical simulators for geothermal reservoirs have been developed. The general purpose of these is to aid reservoir engineers in (i) determining characteristic parameters of reservoirs (most important among those being the reserves of fluid and heat), and (ii) simulating the performance of reservoirs upon production and injection.

The various simulators differ in the approximations made in the underlying physical model (e.g., dependence of rock and fluid properties upon thermodynamic variables), in the geometrical definition of the reservoir (one-, two-, or three-dimensional, regular or irregular shape), in the choice of thermodynamic variables, and in the mathematical techniques used for solving the coupled mass and energy transport equations,

Criteria for desirable performance of numerical simulators depend in part upon the particular problems to be investigated. Different problems will often differ in the required level of detail to be resolved, and in the optimum balance of speed and accuracy of computation. Much can be learned about two-phase flow in porous media from model studies for idealized systems. Such studies can be performed with less-than-three-dimensional models, and algorithms which are based on regular grid spacings will be perfectly acceptable. For modeling natural geothermal reservoirs, on the other hand, it is important that irregular three-dimensional geometries may be handled easily.

In comparison with other two-phase simulators which have been discussed in the literature; the main distinctive feature of SHAFT78 is that it uses an integrated finite difference method (IFD). We solve finite difference equations that are obtained by integrating the basic partial differential equations for mass and energy flow over

discrete surface and volume elements. This method is as easily applicable to irregular geometries of actual reservoirs as it is to idealized, regular geometries; yet the relative simplicity of the finite difference method is retained in the theory and algorithms.

The purpose of this paper is to give a brief review of the basic concepts associated with SHAFT78 and the IFD approach, and *to* present comparisons of SHAFT78 calculations with some analytical solutions. The comparisons include both single-phase and two-phase water problems and demonstrate the accuracy and calculational stability of the algorithm.

The governing equations for mass and energy transport in porous media when both rock and fluid are in local thermodynamic equilibrium can be written

$$\frac{\partial \phi \rho}{\partial t} = -\vec{\nabla} \cdot \vec{F} + q \qquad \text{(1a) (Mass)}$$

$$\frac{\partial U_{vol}}{\partial t} = -\vec{\nabla} \cdot [\vec{F}_\ell H_\ell + \vec{F}_v H_v - KVT] + \{[\frac{\vec{F}_v}{\rho_v} + \frac{\vec{F}_\ell}{\rho_\ell}] \nabla P + \text{dissipative}) + Q \qquad \text{(1b) (Energy)}$$

$$\vec{F} = -k [\frac{k_\ell}{\mu_\ell} \rho_\ell (\nabla P - \rho_\ell \vec{g}) + \frac{k_v}{\mu_v} \rho_v (\nabla P - \rho_v \vec{g})] \qquad (2)$$

Under suitable assumptions, we get the integrated form of equations (1)

$$\frac{d}{dt} \int_V \phi \rho dV = \int_A \vec{F} \cdot \vec{n} da + \int_V q dV \quad (\vec{n} \text{ the inward normal}) \qquad (3a)$$

$$\frac{d}{dt} \int_V U dV = \frac{\int_A \{\vec{F}_\ell H_\ell + \vec{F}_v H_v - \vec{F} U_{ave} - K\nabla T\} \cdot \vec{n} da + \int_V (Q - Uq) dV}{\{\phi \rho + (1-\phi) c_{rock} \rho_{rock} [(\frac{\partial T}{\partial U})_\rho + (\frac{\partial T}{\partial \rho}) \frac{(\partial \rho / \partial t)}{U(\partial U / \partial t)}]\}_{ave}} \qquad (3b)$$

The solution to equations (3) is computed on a polyhedral partitioning of the reservoir whose connected components share a common

polygonal interface. Volume and interface averages are computed using standard finite difference techniques.[1,2] The fluid parameters are obtained by bilinear interpolation (triangular interpolation near the saturation line and in the liquid region)[1] using an inverted form of the 1967 ASME Steam Tables.

It is clear on examination that equations (3) are nonlinear and coupled. These are solved by reduction to an appropriate linear approximation at each time step. Accuracy controls are set to allow only small variations in all parameters over a given time step. The energy equation is solved first using density changes predicted by the behavior of the system in the previous time step. Thus, a good estimate for the expected change of fluid energy over the energy time step can be made, which is subsequently corrected during the density time steps. Special interpol-ation procedures and automatic time-step controls ensure high accuracy of the calculation even when phase transitions occur (elements crossing the saturation line).[2]

An iterative strategy is employed in solving the discretized version of equations (3) after the first-order explicit solution has been generated in each time step. The time-averaged flux terms F (density) or $F_\ell H_\ell + F_v H_v - F U_{ave}$ (energy) are written as

$$\bar{F} = \bar{F}(t + \theta\Delta t) = \bar{F} + 0\Delta t \frac{\partial F}{a t} \qquad (4)$$

and an iteration is performed over the whole mesh to minimize the residual term.[1,8]

SAMPLE PROBLEMS

In order to evaluate the SHAFT78 program, calculated results were compared to numerical calculations reported in the literature (e.g., Toronyi[7] and Garg[5]), and to analytic solutions. The remainder of this paper is devoted to a comparison of the computed solutions with the analytic results.

SINGLE-PHASE VAPOR

In 1957 R.E. Kidder presented to the ASME[3] the solution to the problem of isothermal flow of a gas (obeying Darcy's and Boyle's laws) in the semi-infinite homogenous porous solid.

Specifically, the problem solved was

$$\frac{\partial}{\partial x}\left[p\,\frac{\partial p}{\partial x}\right] = \phi\,\frac{\mu}{k}\,\frac{\partial P}{\partial t} \qquad (5)$$

with initial conditions

$$P(x,0) = Po \quad 0 < x < \infty \qquad (6)$$

and boundary conditions

$$P(0,t) = P_1 < Po \quad 0 < t < \infty \qquad (7)$$

SHAFT78 was run on a 30-element linear mesh with internode distances of .2m, and large nodes at the boundaries of the grid with the appropriate boundary conditions. Initial conditions were

P_o = 5MPa
T_o = 300 ^{o}C

with rock properties

$k = 10^{-12}$ m^2, $K_{rock} \sim 0$, c_{rock} = 107 J/kgoC, ρ_{rock} = 2200 kg/m3, ϕ = .2

Three boundary conditions on the left of the grid

P_1 = 4MPa
P_1 = 2MPa
P_1 = 1MPa

were chosen and the results are compared with the analytic solution for each case in Figure 1.

The computed solution shows a slightly lower pressure drop than the analytic solution; This is probably due to inaccuracies introduced in the boundary approximations.

SINGLE-PHASE LIQUID

To evaluate the performance of **SHAFT78** in the liquid region, the "Theis problem"[4] was run on a 15-element mesh with a large element at the outer boundary to simulate the reservoir conditions at infinity.

Reservoir conditions were

Thickness	= 100 m
Initial pressure	= **20.37** MPa
Initial temperature	= 180 ^{o}C
Rock porosity	= .2
Permeability	= 10^{-13} m^2
Rate of fluid withdrawal	= 18 kg/s·m

The results are compared in Figure **2** to the analytic solution of the line source problem (t_D vs P_D on a log-log scale)

$$\nabla^2 P = \frac{\phi \mu c}{k} \frac{\partial P}{\partial r} \qquad (8)$$

$$P(r,o) = P_o \quad \text{initial conditions} \qquad (9)$$

$$\lim_{r\to\infty} P(r,t) = P_o$$

$$\lim_{r\to\infty} \frac{2\pi r k}{\mu} \frac{\partial p}{\partial r} = -q \quad \text{boundary conditions (Constant flux with Darcy assumption)} \qquad (10)$$

with solution given by the exponential integral

$$P = P_o + \frac{q\mu}{4\pi k} Ei\left\{\frac{-r^2}{4t} \frac{\phi \mu c}{k}\right\} \qquad (11)$$

Agreement is close near the sink (to the right of the plot) with deviations increasing to the left. The scatter of computed points around the analytic solution seems to reflect a deviation from the

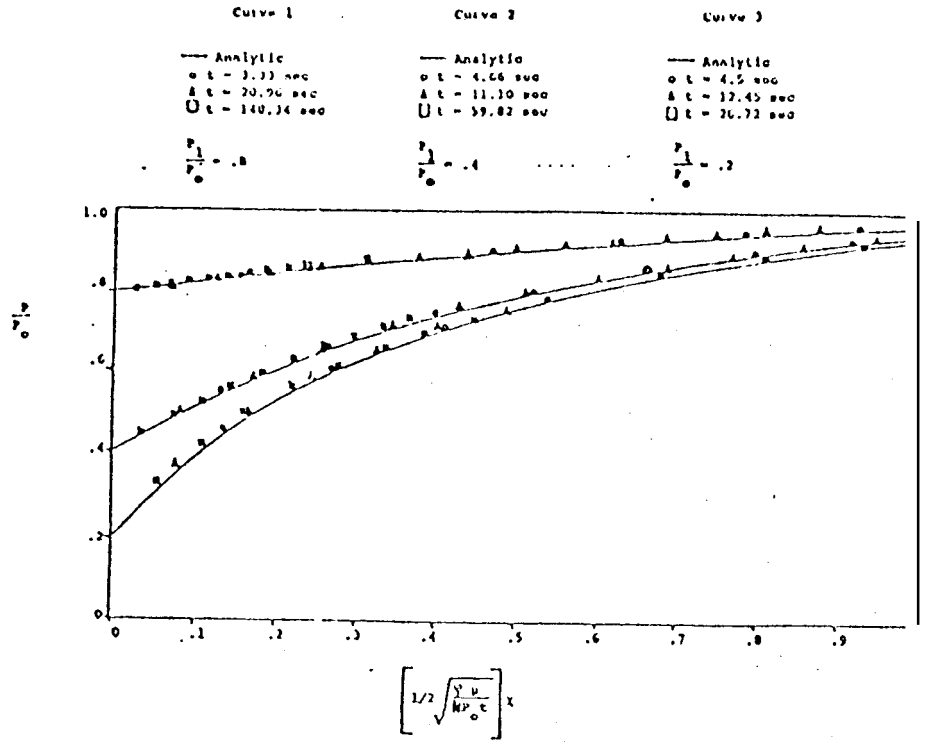

FIGURE 1

.KIDDER PROBLEM **ANALYTIC VS. COMPUTED SOLUTION**

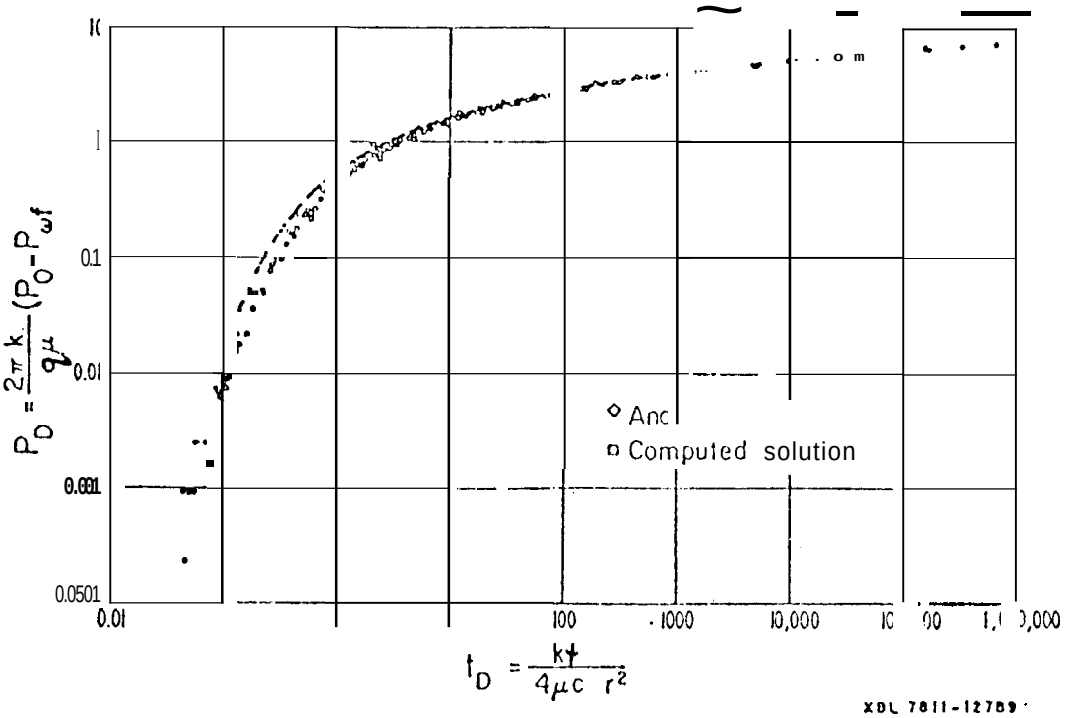

FIGURE 2

THEIS **PROBLEM ANALYTIC VS. COMPUTED SOLUTION**

solution at late times and large radius when the boundary approximation becomes less accurate.

TWO-PHASE RESERVOIR

Garg derives an approximate diffusivity equation[5] for pressure in a two-phase reservoir initially at equilibrium pressure p_o, which is valid near the wellbore.

$$\frac{\partial P}{\partial t} - \frac{(k/\nu)_T}{\phi \rho C_T} [\nabla^2 P] = 0 \qquad (12)$$

Here we have introduced the total kinematic mobility

$$(\frac{k}{\nu})_T = k[\frac{k_\ell}{\mu_\ell} \rho_\ell + \frac{k_v}{\mu_v} \rho_v]. \qquad (13)$$

For a line source, we have the boundary conditions at the well

$$r \frac{\partial P}{\partial r}\Big|_{r=r_w} = - \frac{q}{2\pi(k/\nu)_T} \qquad (\nu \equiv \frac{\mu}{\rho}) \qquad (14)$$

and at infinity

$$\lim_{r \to \infty} P(r,t) = P_\theta \qquad (15)$$

The solution (after Carslaw and Jaeger) to the above equation is

$$P(r,t) = P_o + \frac{q}{4\pi(k/\nu)_T} \, Ei \{- \frac{r^2}{4t} \frac{\phi \rho C_T}{(k/\nu)_T}\} \qquad (16)$$

For sufficiently large t (argument of the exponential integral less than 10^{-2}) we have for the wellbore pressure[5]

$$p_w(t) = P(r_w,t) = P_o - \frac{1.15q}{2\pi(k/\nu)_T} \{\log_{10}(\frac{t(k/\nu)_T}{\phi r_w^2 \rho C_T}) + .351\} \qquad (17)$$

This implies that a plot of P_w vs. log t should be a straight line, with slope equal to $1.15q/2\pi(k/\nu)_T$.

SHAFT78 was used to simulate the problem of a mass withdrawal of .14 kg/s·m on a radial grid identical to that reported by Garg[5] with

$$Ar_1 = Ar_2 = \ldots Ar_{11} = 1\,m$$

$$Ar_{12} = 1.2\Delta r_{11}, \ldots, \Delta r_{50} = 1.2\Delta r_{49}$$

using rock properties

$$\rho_{rock} = 2.65 \times 10^3 \text{ kg/m}^3$$

$$\phi = .2$$

$$c_{rock} = 1000 \text{ J/kg·}^{o}\text{C}$$

$$K_{rock} = 5.25 \text{ W/m·}^{o}\text{C}$$

Permeability (k) = 10^{-13} m^2 (100 millidarcy)

The relative permeability curves used[6] for the simulation are shown in Figure 6A.

Results of our simulations for three different initial conditions are given in Table 1 and Figures 3-5. P is seen to be a linear function of log t, the slope of which gives a good estimate of the total kinematic mobility $(k/\nu)_T$. We have also plotted P vs $\log(t/r^2)$ for the same simulations, but including all elements, not just the wellblock (Figures 3B, 4B, 5B). Again a straight line results, with slope almost identical to that of the P vs. log t plots. This result, which is outside the scope of Garg's theory, seems to indicate that total kinematic mobilities could also be obtained from observation well data rather than just from flowing wellbore data.

In addition, saturation vs log (t/r^2) was plotted for 3 times for each of the three cases just discussed. As can be seen in Figure 7, saturation appears to be a function of t/r^2 only. At a position proportional to $\sqrt{t}$ there appears a broad saturation front, which becomes more diffuse as vapor saturation increases. Changing the relative permeability curves (Figure 6B) has only a slight effect on the saturation profiles. We are still investigating these results.

Table 1

Results for Total Kinematic Mobilities $(k/\nu)_T$

Initial saturation (S_o) and pressure (P_o)	$(k/\nu)_T$ from P vs log(t) plot	$(k/\nu)_T$ from P vs log (t/r^2) plot	Time (sec)	Actual value of $(k/\nu)_T$
a_o = æ ϶ MPa S_o = 9	2 ƶ1⊂6 x 10^{-7}	2 4265 × 10^{-7}	0. 1889. 7490. 10184.	2.3117 × 10^{-7} 2.2119 × 10^{-7} 2.2154 × 10^{-7} 2.2105 × 10^{-7}
P_o = 8 6 MPa S_o = ϶	1 1610 x 10^{-7}	1 ≥2ϕ6 × 10^{-7}	0. 3775. 7033. 19268. 45883.	1.2633 x 10^{-7} 1.1596 x 10^{-7} 1.1479 x 10^{-7} 1.1404 x 10^{-7} 1.1314 x 10^{-7}
P_o = 8 6 MPa S_o = .1	3 æƶ39 × 10^{-7}	⊂ 161 x 10^{-7}	0. 2336. 19327. 76549. 142060. 217406.	5.5535 x 10^{-7} 4.0947 x 10^{-7} 3.9253 x 10^{-7} 3.8568 x 10^{-7} 3.7956 x 10^{-7} 3.7866 x 10^{-7}

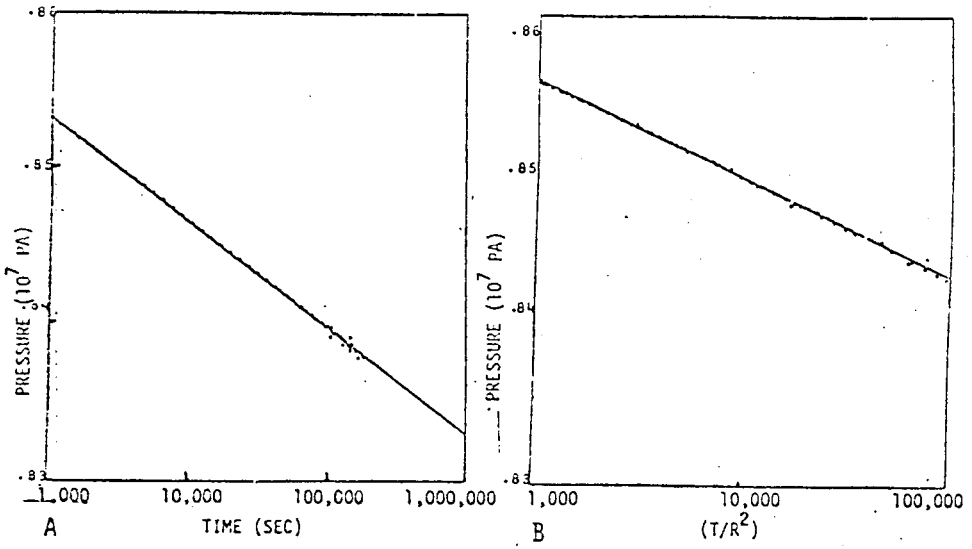

FIGURE 3. GARG PROBLEM - INITIAL RESERVOIR SATURATION = .1

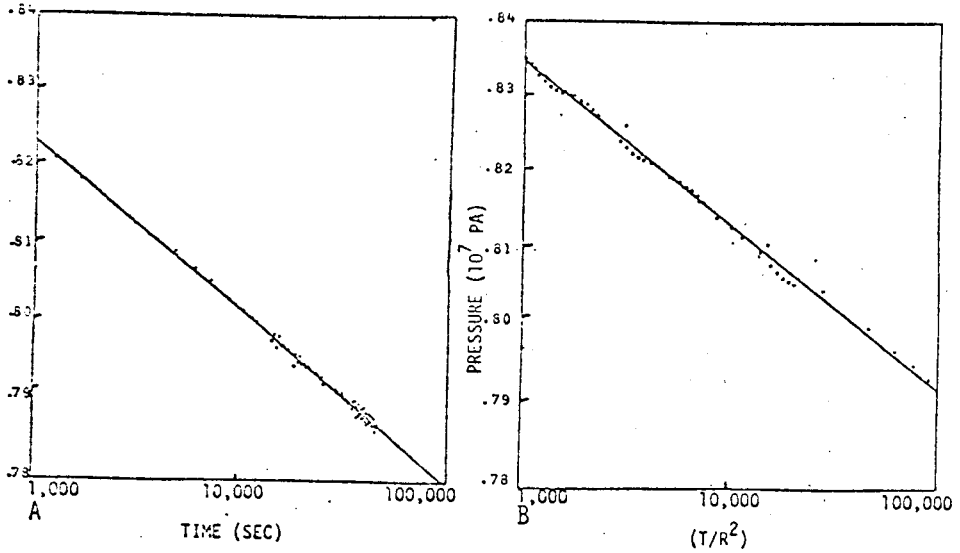

FIGURE 4. GARG PROBLEM - INITIAL RESERVOIR SATURATION = .5

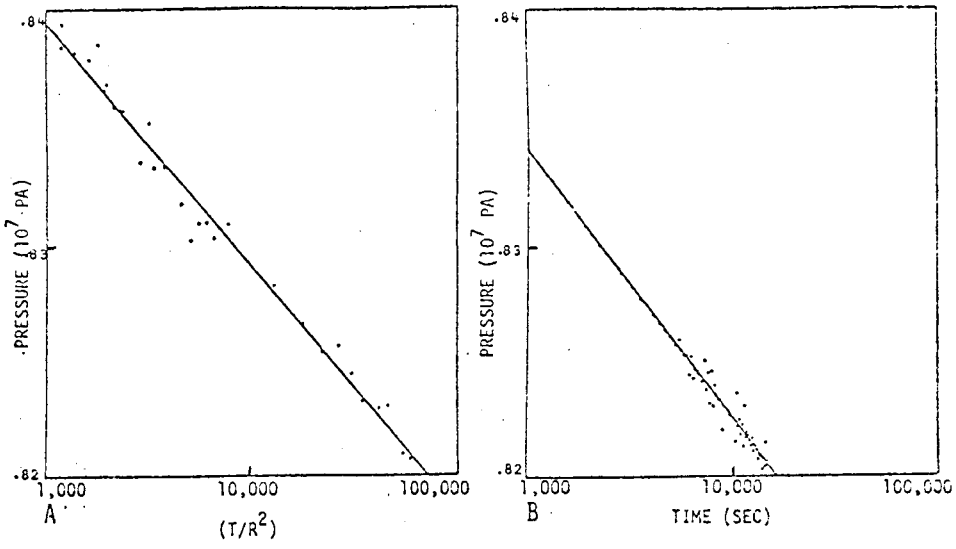

FIGURE 5. GARG PROBLEM - INITIAL RESERVOIR SATURATION = .9

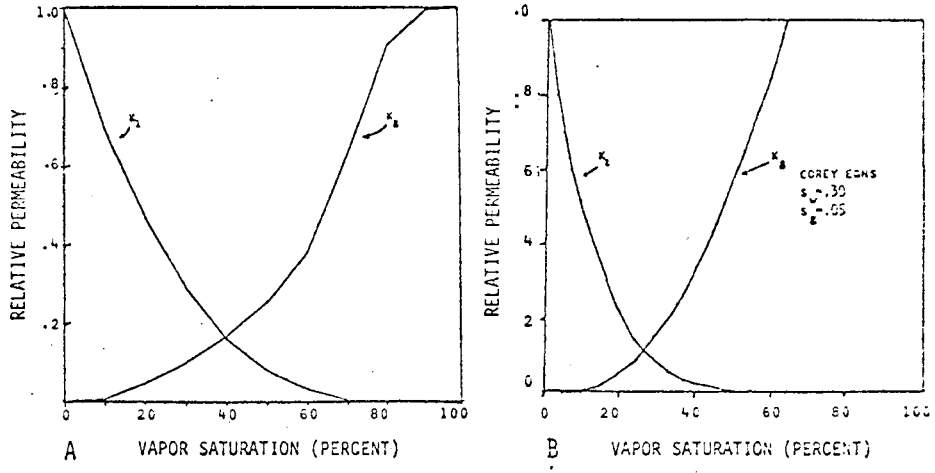

FIGURE 6. RELATIVE PERMEABILITY CURVES

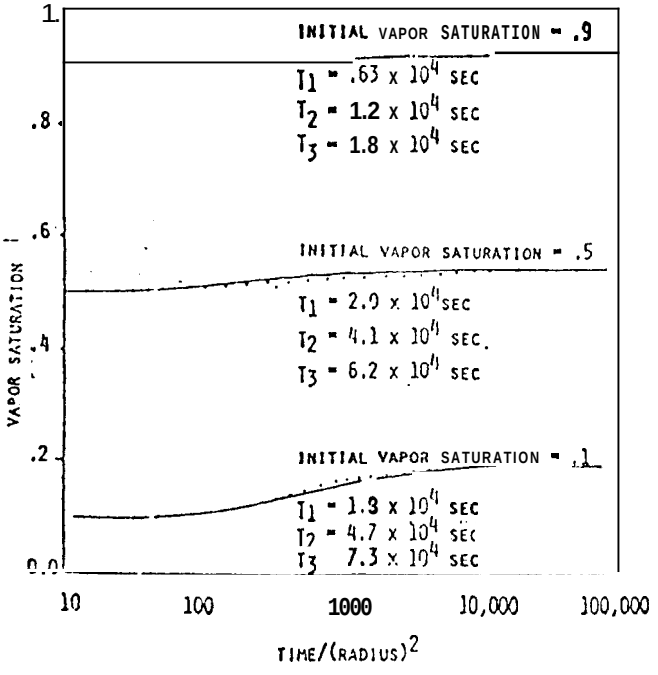

FIGURE 7. PLOT OF VAPOR SATURATION VS. T/R^2 ON A LOG-LINEAR SCALE FOR GARG PROBLEM,

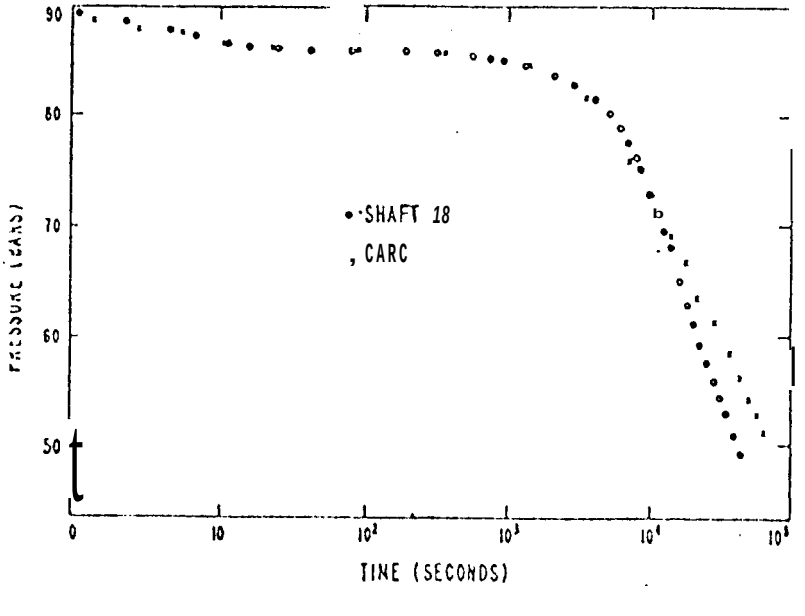

FIGURE 8. DRAWDOWN FROM AN INITIALLY LIQUID RESERVOIR WITH A PROPAGATING TWO-PHASE REGION.

Program SHAFT78 was also run to simulate a drawdown from a liquid reservoir with initial conditions

$$T_o = 300\ ^oC$$

$$P_o = 9.0\ MPa$$

$$k = 10^{-14}\ m^2$$

and the results are compared with Garg's reported results in Figure 8.

For this comparison, the Corey equation was used to generate the relative permeability curves with the parameters

$$S_w = .3$$

$$S_g = .05$$

From the slope of the straight line portion of the curve we compute a $(k/\nu)_T$ value of .86E-8 as compared to numerical values ranging from 1.4E-8 to 1.9E-8. However, $(k/\nu)_T$ values computed from the numerical simulation are decreasing with increasing time, while the straight line portion of the curve appears to be flattening out as time progresses. Thus, it appears that the computed $(k/\nu)_T$ values are converging to the numerically generated values as the flash front passes through the grid blocks.

CONCLUSION

The simulator SHAFT78 has been verified for a number of one- and two-phase flow problems involving subcooled water, water/steam mixtures, and superheated steam. The flow of water and steam in porous media, boiling and condensation, and heat exchange between rock and fluid are all described properly. No difficulties are encountered in crossing the saturation line (phase transitions).

Our simulation results confirm Garg's method of deducing total kinematic mobilities in two-phase reservoirs from production well pressure decline. It is suggested that total kinematic mobilities can also be inferred from observation well data. For uniform initial conditions we observe a simple dependence of vapor saturation upon production time and upon distance from the producing well. This as yet unexplained phenomenon indicates an underlying simplicity of two-phase porous flow,

Apart from idealized model studies, SHAFT78 is also being used for irregular three-dimensional systems. A simulation of production and recharge in the Krafla geothermal field (Iceland) is reported elsewhere.[9] At present, we are developing a history match for production and injection in the highly irregular shaped field of Serrazzano (Italy).[10]

REFERENCES

1. Pruess, K, R. Schroeder, P. Witherspoon, J. Zerzan. "SHAFT78, A Two-Phase Multidimensional Computer Program for Geothermal Reservoir Simulation," (LBL-8264)

2. Pruess, K, R. Schroeder, P. Witherspoon, J. Zerzan. "Description of the 3-D 2-Phase Simulator SHAFT78 for use in Geothermal Reservoir Studies," (SPE-7699), paper to be presented at the 5th SPE-Symposium on Reservoir Simulation, Denver, 31 January—2 February (1979).

3. Kidder, R. 1957, "Unsteady Flow of Gas through a Semi-Infinite Porous Medium," presented at Applied Mechanics Division Summer Conference, Berkeley, California, Paper #57.

4. Matthews, C.S. and D.G. Russell, 1967, "Pressure Build-Up and Flow Tests in Wells," SPE Monographs.

5. Garg, S.K., 1978, "Pressure Transient Analysis for Two-Phase (Liquid Water/Steam) Geothermal Reservoirs," SSS-IR-78-3568(R2).

6. Muskat, M., R.D. Wyckoff, H.G. Botset, and M.W. Meres, 1937, "Flow of Gas-Liquid Mixtures through Sands," Trans. AIME, 123, p. 69.

7. Toronyi, R.M. and S.M. Farouq Ali, 'Two-Phase, Two-Dimensional Simulation of a Geothermal Reservoir," Soc. Pet. Eng. J. (June 1977) 171-183.

8. Lasseter, T.J., P.A. Witherspoon, and M.J. Lippmann, "Multiphase Multidimensional Simulation of Geothermal Reservoirs," Proceedings Second United Nations Symposium on. the Development and Use of Geothermal Resources, San Francisco, Calif. (1975) vol. 3, 1715-1723.

9. Jonsson, V., "Simulation of the Krafla Geothermal Field," Lawrence Berkeley Laboratory Rept. LBL-7076, Berkeley, Calif. (1978).

10. Weres, O., "A Model of the Serrazano Zone," Proceedings Third Stanford Workshop on Geothermal. Reservoir Engineering, Stanford, Calif. (1977) 214-219.

NOMENCLATURE

Latin — Upper Case

C_T = total compressibility
F = mass flux per unit area, kg/m^2s
H = enthalpy per unit mass, J/kg
K = rock heat conductivity, $J/ms\ ^oC$
P = pressure, Pa = N/m^2
P_D = dimensionless pressure
P_w = wellbore pressure, N/m^2
P_o = initial pressure, N/m^2
Q = energy source term, J/m^3s
T = temperature, ^oC
U = energy per unit mass (specific energy), J/kg
U_{vol} = energy per unit volume, J/m^3
S = volumetric vapor saturation

Latin — Lower Case

c = rock specific heat, $J/^oC\ kg$
k = absolute permeability, m^2
$(k/\nu)_T$ = total kinematic mobility, s
q = mass source term, kg/m^3s
r_w = wellbore radius, m
t = time, s

Greek

Θ = time averaging factor (dimensionless)
ρ = density, kg/m^3
ϕ = rock porosity, dimensionless
μ = dynamic viscosity, Ns/m^2
ν = kinematic viscosity, Nsm/kg

Subscripts

ave = average (over volume or surface element)
ℓ = liquid component
rock = referring to rock
v = vapor component
vol = volumetric measurement of the variable
(*e.g.*, U_{vol} = Energy/unit volume).